academicJournals

Vol. 14(33), pp. 2554-2567, 19 August, 2015
DOI: 10.5897/AJB2015.14692
Article Number: EBC7E4F54969
ISSN 1684-5315

http://www.academicjournals.org/AJB

African Journal of Biotechnology

Full Length Research Paper

Biosynthesis of silver nanoparticles by plants crude extracts and their characterization using UV, XRD, TEM and EDX

Vishwajeet Singh[1*], Ankita Shrivastava[2] and Nitin Wahi[3]

[1]Department of Botany, Raja Balwant Singh, College, Dr B.R. Ambedkar University, Agra-282002, U.P., India.
[2]New Era Research Foundation, Agra-282007, India, U.P., India.
[3]Department of Biotechnology, GLA University, Mathura-281406, U.P., India.

Received 4 May, 2015; Accepted 13 July, 2015

Plant extracts are very cost effective and eco-friendly, thus, can be an economic and efficient alternative for the large-scale synthesis of nanoparticles. The preparation of stable, uniform silver nanoparticles by reduction of silver ions with *Emblica officinalis*, *Terminalia catappa* and *Eucalyptus hybrida* extract is reported in the present paper. It is a simple process of global research interest for obtaining silver nanoparticles in least amount of time. These nanoparticles were characterized with UV-Vis spectroscopy, X-ray diffraction (XRD), transmission electron microscopy (TEM) and energy diffraction X- ray (EDX analysis which revealed that the silver nanoparticles are polydisperse and of different morphologies ranging from 20 to 80 nm in size. XRD results reveal that these nanostructures exhibit a face-centered cubic crystal structure. The UV/Vis spectra absorption peak confirms their production. Pioneering of reliable and eco-friendly process for synthesis of metallic nanoparticles biologically is an important step in the field of application of nanobiotechnology. Thus, these silver nanoparticles (Ag-NPs) may prove as a better candidate for drugs and can potentially eliminate the problem of chemical agents because of their biogenic nature. The indiscriminate use of antibiotics has fuelled the development of drug resistance at an alarming rate. To overpower this burning problem, the Ag-NPs may prove to be a universal solution.

Key words: Nanobiotechnology, silver nanoparticles (Ag-NPs), *Emblica officinalis*, *Terminalia catappa* and *Eucalyptus hybrida.*

INTRODUCTION

Nanotechnology (NT) is the engineering of functional systems at the molecular scale. NT is the ability to work at the atomic, molecular and supramolecular levels (on a scale of 1 to 100 nm) in order to understand, create and use material structures, devices and systems with fundamentally new properties and functions resulting from their small structure. NT provides the tools and technology platforms for the investigation and trans-

*Corresponding author. E-mail: officervishu@gmail.com. Tel: 8410829626.

formation of biological systems, and biology offers inspiration models and bio-assembled components to NT (Mihail, 2003). Silver is used in the medical field as a topical bactericide (Yamanaka et al., 2005). With the progress of NT, production of the nanoparticle possesses more surface atoms than microparticles, which greatly improves the particles physical and chemical characteristics. There are some physical and chemical methods available for silver nanoparticle (Ag-NP) synthesis but these are so tedious; they consume lot of energy to maintain high pressure and temperature. Involvement of toxic chemicals in the synthesis process may be harmful to human beings (Chen et al., 2003). With the emergence and increase of microbial organisms resistant to multiple antibiotics, and the continuing emphasis on health-care costs, many researchers have tried to develop new, effective antimicrobial reagents free of resistance and cost. Recently, resistance to commercially available antimicrobial agents by pathogenic bacteria and fungi is increasing at an alarming rate and has become a global threat. Drug resistance is one of the most serious and widespread problems in all developing countries (Stevanovic et al., 2012). Such problems and needs have led to the resurgence in the use of Ag-based antiseptics that may be linked to broad-spectrum activity and far lower propensity to induce microbial resistance than antibiotics (Jones et al., 2004). The antibacterial effects of Ag salts have been noticed since antiquity (Silver and Phung, 1996), and Ag is currently used to control bacterial growth in a variety of applications, including dental work, catheters, and burn wounds (Catauro et al., 2004; Crabtree et al., 2003). In fact, it is well known that Ag ions and Ag-based compounds are highly toxic to microorganisms, showing strong biocidal effects on as many as 12 species of bacteria including *Escherichia coli* (Zhao and Stevens, 1998).

The development of cost efficient and ecologically benign methods of synthesis of nanomaterials still remains a scientific challenge as metal nanoparticles are of use in various catalytic applications, viz electronics, biology and biomedical applications, material science, physics, environmental remediation fields (Gonzalez and Noguezm, 2007; Gross et al., 2007; Kim et al., 2003; Parak et al., 2003; Schultz, 2003; Smith et al., 2006; Wei et al., 2005; Wang et al., 2007). It is well known that the toxicity of nanomaterials essentially depends on the structural features such as size, shape, composition and the surface chemistry. To prolong the life span of metal nanoparticles it is vital to select stabilizing agents and pathways that are environmentally friendly, non-toxic and easy to implement. Novel methods of ideally synthesizing NPs are thus being thought which are formed at ambient temperatures, neutral pH, low costs and environmentally friendly fashion. Keeping these goals in view nano-materials have been synthesized using various routes. Among the biological alternatives, plants and plant extracts seem to be the best option. In this paper, we report a green method for the synthesis of silver nanoparticles at room temperature by using plant extracts of *Emblica officinalis*, *Terminalia catappa* and *Eucalyptus hybrida*. These nanoparticles were characterized with UV-Vis spectroscopy, XRD, TEM and EDX analyses. Furthermore, we will use these Nanoparticles to evaluate *in-vitro* antimicrobial activity for the development of nanosilver-phytochemical composite formulation.

MATERIALS AND METHODS

Synthesis of silver nanoparticles using leaves extract of *E. officinalis, E. hybrida and T. catappa*

Fresh leaves of *E. officinalis, E. hybrida* and *T. catappa* were collected and were washed thoroughly with distilled water. About 50 g of leaves were cut into small pieces. Finely cut leaves were dipped into a beaker containing 200 ml distilled water. After that the mixture was boiled for 10 to 12 min. The extract was filtered using Whatmann filter paper and filtrate was collected. Synthesis of silver nanoparticles using extract of these leaves was mixed with aqueous solution of 1 mM Silver nitrate (99.99%) in 1:4 ratios in conical flask under aseptic conditions. The pH was adjusted to 8.0. The conical flasks were then agitated at 100 rpm in dark at 25°C on shaker for 1 to 2 h. A change in the color of the solution was observed. Control set (only extract) without $AgNO_3$ was also run side by side. Another negative control containing only 1 mM $AgNO_3$ were maintained under the same conditions. Silver nanobioconjugates were characterized by various methods.

Characterization of the synthesized silver nanoparticles

UV–visible spectroscopy

The detection of Ag-NPs was primarily carried out by visual observation by colour change of the cell filtrate after treatment with silver nitrate (1 mmol $^{-l}$). A further characterization of synthesized Ag-NPs was carried out with the help of UV–Visible spectrophotometer by scanning the absorbance spectra in 250 to 800 nm range of wavelength. It was observed that upon addition of the extract into the flask containing the aqueous silver nitrate solution, the colour of the medium changed to brown within 2 min. This indicated the formation of silver nanoparticles. The solution containing the signatory colour of AgNPs (dark brown) was then poured out into Petri-dishes and left in the oven for drying at 50°C for 24 h. The formation and quality of compounds were checked by XRD technique. The X-ray diffraction (XRD) pattern measurements of drop- coated film of AgNPs on glass substrate were recorded in a wide range of Bragg angles θ at a scanning rate of 2° min^{-1}, carried out on a XRD Diffractometer (PANalytical-XPERT PRO diffractometer system) that was operated at a voltage of 40 kV and a current of 30 mA with CuKα radiation (1.5405 Å). High Resolution Transmission Electron Microscopy (HRTEM) was per- formed by TECHNAIG20-STWIN (200 KV) machine with a line resolution 2.32 (in angstrom). These images were taken by drop coating AgNPs on a carbon-coated copper grid. Energy Dispersive Absorption Spectroscopy photograph of AgNPs were carried out by the HRTEM equipment.

Scanning electron microscopy

Scanning electron micrographs were taken. Samples were

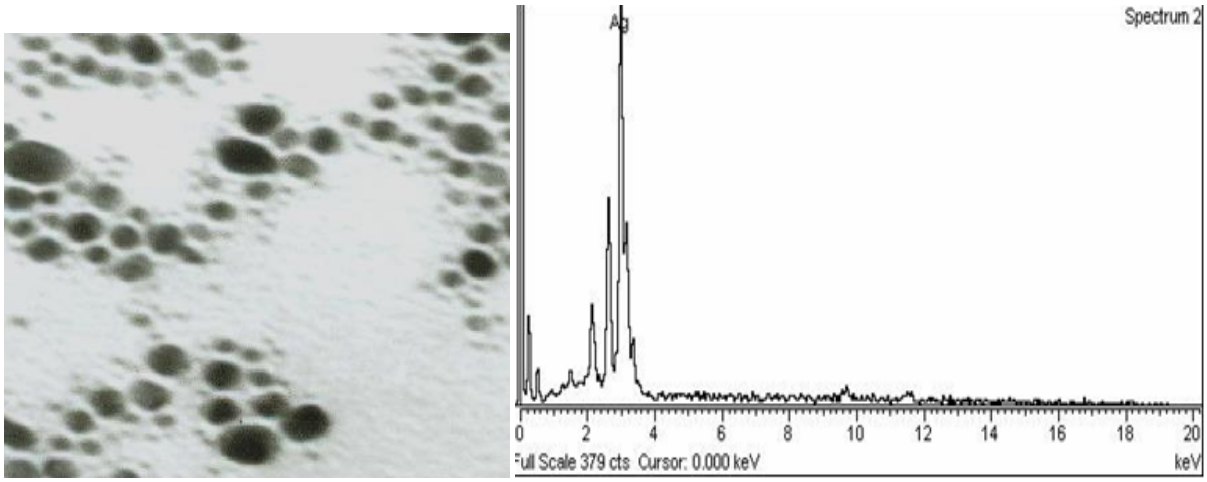

Figure 1. Synthesis of nanoplates by crude *Emblica*, (80 to 300 nanometers) of silver by reducing Ag ions EDX spectrum recorded from drop-coated films of silver nanoparticles.

prepared by fixing with 2Æ5% glutaraldehyde overnight at room temperature. The fixed sample was dehydrated with gradient alcohol (10 to 95%), incubated for 20 min in each gradient and dipped in absolute alcohol for 2 to 5 min. Finally, specimen was prepared by placing a drop of dehydrated sample on a glass slide, followed by coating with monolayer platinum for making the surface conducting.

XRD measurements

The purified powders of silver nanoparticles of varying interaction times were subjected to XRD measurements using an XRD Diffractometer (PANalytical-XPERT PRO diffractometer system). The target was Cu K α with a wavelength of 1.54060 A°. The generator was operated at 40 kV and with a 30 mA current. The scanning range was selected between 10 and 100°C. The crystallite size was also determined using the Debye Scherrer equation.

Transmission electron microscopy (TEM)

The samples for transmission electron microscopy (TEM) analysis were prepared by drop-casting the Silver Nano Bio Conjugates solution on a carbon-coated copper TEM grid. Before casting to the grid the Silver Nano Bio Conjugates solution was centrifuged at 10000 rpm for 5 min and the isolated silver Nano Bio Conjugates were dispersed in 100 µl double distilled water and sonicated in a bath sonicator for 15 min. The TEM images were recorded on a high resolution electron microscope (HRTEM: JEOL JEM 2010) operating at an accelerating voltage of 200 kV. Fast Fourier transform (FFT) images were recorded with built-in software for the FFT algorithm for image processing in HRTEM: JEOL JEM 2010 instrument at NPL, New Delhi.

Energy diffraction X- ray (EDX) measurements

The EDX analysis was carried out using JEOL JSM 7600F.

Fourier transform infrared spectroscopy

For FTIR spectrum analysis the silver nano bioconjugates were centrifuged at 15,000 rpm for 15 min to remove free proteins or other compounds present in the solution. The filtrate after complete reduction of Ag+ ions was subjected to repeated centrifugation at 15,000 rpm for 15 min, and supernatant was replaced by distilled water each time to concentrate Ag-NPs. The process was repeated for three times and finally the centrifuged part containing silver nano bioconjugates were redispersed in double distilled water and subjected to FTIR spectroscopy. The presence of unreacted silver ions leads to white precipitation on addition of sodium chloride. However, no precipitate was formed after addition of sodium chloride indicating the absence of unreacted silver in the nanoparticle solution. FTIR measurements were carried out to identify the possible biomolecules responsible for the reduction of the Ag+ ions and capping of the bioreduced silver nanoparticles synthesized by the leaf broth. The Fourier transform infrared spectroscopy (FTIR) spectrum of the sample was recorded on a Perkin-Elmer FTIR spectrum in the range 450 to 4000 cm^{-1} at resolution of 4 cm^{-1}.

RESULTS AND DISCUSSION

Synthesis of silver nanoparticles using leaves extract of *E. officinalis, E. hybrida* and *T. catappa*

Synthesis of silver nanobioconjugates was done using leaves extract of *E. officinalis, E. hybrida* and *T. catappa.* By *Emblica* crude *emblica*, synthesis of nanoplates (80 to 300 nm) of silver by reducing Ag ions EDX spectrum was recorded from drop-coated films of silver nanoparticles (Figure 1). UV-vis spectra was recorded from the aqueous silver nitrate and *E. hybrida* leaf extract. It was observed that the silver surface plasmon resonance band occurs at 440 nm and steadily increases in intensity as a function of time of reaction without any shift in the peak wavelength (Figure 2). The frequency and width of the surface plasmon absorption depends on the size and shape of the metal nanoparticles as well as on the dielectric constant of the metal itself and the surrounding medium. SEM images of reduction of Ag+ to silver

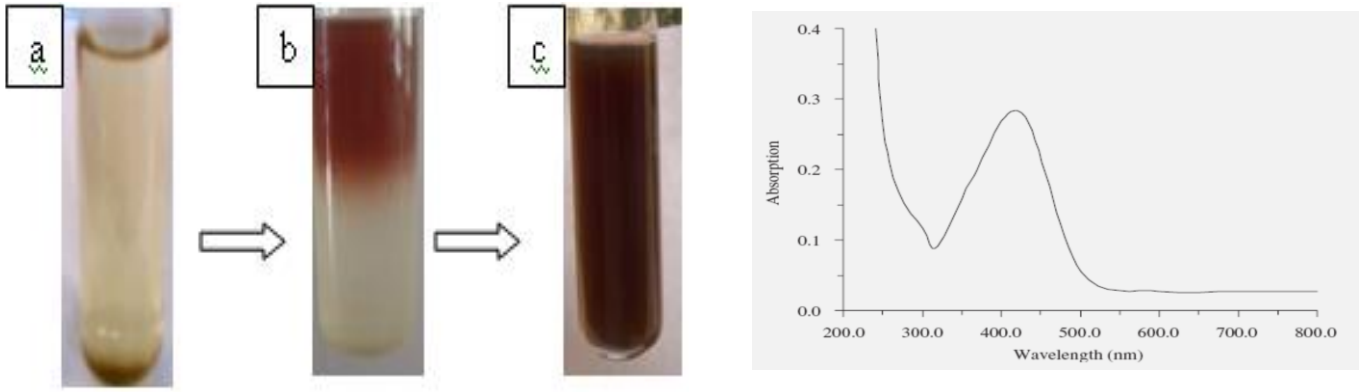

Figure 2. Pictures showing the color changes before (a), during (b) and after the process of reduction of Ag+ to Ag nanoparticles (c).

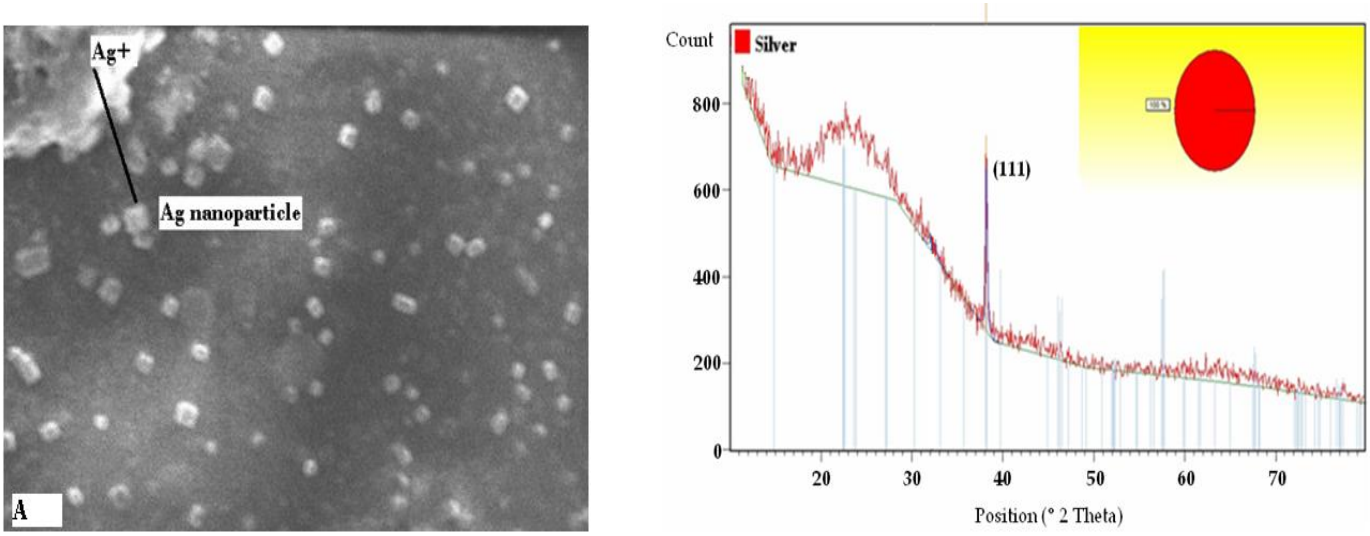

Figure 3. SEM images of reduction of Ag+ to Silver nanoparticles.

nanoparticles in solution by exposing 5 ml of *E. hybrida* leaves extract to 45 ml of 1 mM aqueous $AgNO_3$ at 26°C were done (Figure 4). XRD patterns were recorded from drop-coated films on glass substrate of silver nanoparticles synthesized by treating *E. hybrida* leaf extract with $AgNO_3$ aqueous solutions. The Bragg reflections are indexed on the basis of the fcc silver structure. XRD patterns obtained for silver nanoparticles synthesized using *E. hybrida* leaf extract in Figure 3, it shows characteristic peaks (at $2\theta = 30.8°$), marked with (111). A number of Bragg reflections corresponding to the (111) sets of lattice planes are observed which may be indexed based on the face-centred cubic structure of silver. The XRD pattern thus clearly shows that the silver nanoparticles are crystalline in nature. The XRD pattern of pure silver ions is known to display peaks at $2\theta = 7.9$, 11.4, 17.8, 30, 38, and 44°. The value of the pure silver lattice constant has been estimated to be a = 4.081, a value that is consistent with a = 4.0862 A° reported by the JCPDS file n^{o}4-0783. This estimation confirmed the hypothesis of particle monocrystallinity. *Terminalia* leaf extract in Figure 5 shows the UV-Vis spectra, EDAX and HR-TEM micrograph of synthesized Ag nanoparticles (20 to 80 Nanometers; spherical and triangle shaped).

Characterisation of silver nanobioconjugates

UV-vis spectroscopy

It is well known that silver nanoparticles exhibit yellowish-brown color in water. These colors arise due to excitation of surface plasmon vibrations in the metal nanoparticles which occur in the range 380 to 440 nm in an aqueous

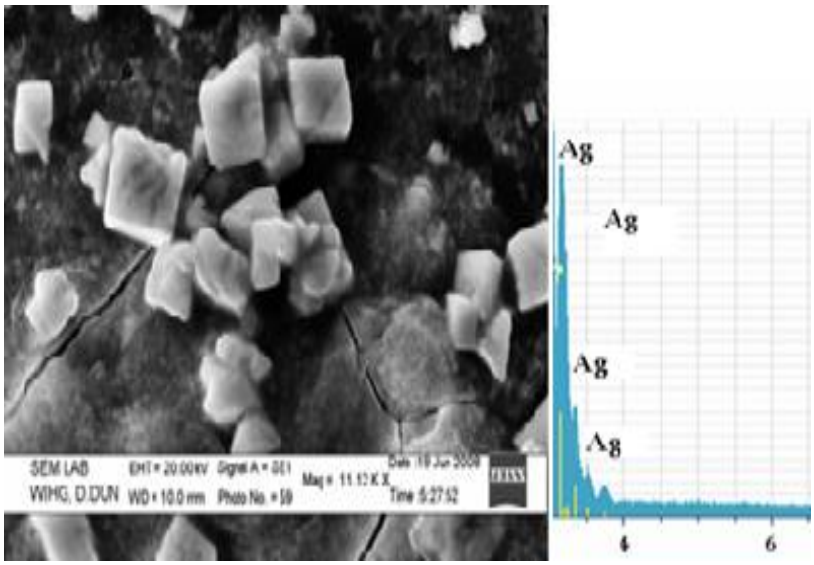

Figure 4. SEM image of the silver nanoparticles synthesized by treating *Eucalyptus hybrida* leaf extract with $AgNO_3$ aqueous solutions. Silver nanoparticles formed were predominantly cubical with uniform size, EDX spectrum recorded from a film, after formation of silver nanoparticles. Different X-ray emission peaks are labelled.

medium. From the inset of Figure 6, it shows that the silver nitrate treated with *E. officinalis*, *E. hybrida* and *T. catappa* biomass turned dark reddish-brown after 1 to 3 h due to the formation of silver nanoparticles extracellularly. This shows that it was a quite fast process. This color is due to the SPR signal generated in the region 340 to 450 nm of silver nano bio conjugates by UV-visible spectroscopy. An increase in absorbance in the region 340 to 450 nm with time indicated the synthesis of Silver Nano Bio Conjugates. However, no change in color was observed in control sets.

The intensity of the surface plasmon band is seen to saturate after 2 h of reaction

XRD measurements

Figure 7 shows the XRD pattern obtained for Silver Nano Bio Conjugates synthesized using the *E. hybrida*, *T. catappa* and *E. officinalis* extract represented by the curve. A number of Bragg reflections are observed for the silver nanoparticles synthesized with each of the *T. catappa* and *E. officinalis* extract, which may be indexed based on the fcc structure of silver and is shown in Table 1. The XRD pattern thus clearly shows that the silver nanoparticles formed by the reduction of Ag+ ions by the *T. catappa*, *E. hybrida*, and *Emblica officinalis* extract are crystalline in nature. From the calculated d spacing values corresponding to each 2θ values, it appears that the (101), (111), (200), and (220) lattice spacing are broadened as compared to the bulk form and this phenomenon is more pronounced in case of the (111) planes. In addition to the Bragg peaks representative of fcc silver nanocrystals (JCPDS—International Center for Diffraction Data, PCPDFWIN v. 1.30, 31-1238) corresponding to the lattice planes (101), (111), (200) and (220), respectively. The XRD pattern of pure silver ions is known to display peaks at 2θ = 7.9, 11.4, 17.8, 30, 32, 38, and 44°. This estimation confirmed the hypothesis of particle monocrystallinity. The sharpening of the peaks clearly indicates that the particles are in the nanoregime. The XRD pattern thus clearly shows that the silver nanoparticles are crystalline in nature.

Transmission electron microscopy (TEM)

Figure 8 shows TEM images recorded from drop-coated films of the Silver Nano Bio Conjugates synthesized with *T. catappa* leaf extract. At low magnification (Figure 8), a very large density of silver nanoparticles can be seen and the silver nanoparticles are quite polydisperse and ranged in size from 10 to 40 nm with an average size ca. 20 nm. At higher magnification, the morphology of the silver nanoparticles is more clearly seen (Figures 8B and C). The particles are predominantly spherical with a small percentage being elongated. The assembly of the silver particles in the manner observed might be driven by the presence of the bioorganic molecules. While the TEM pictures do not provide direct evidence of the presence of a bioorganic material on the silver nanoparticles, it is

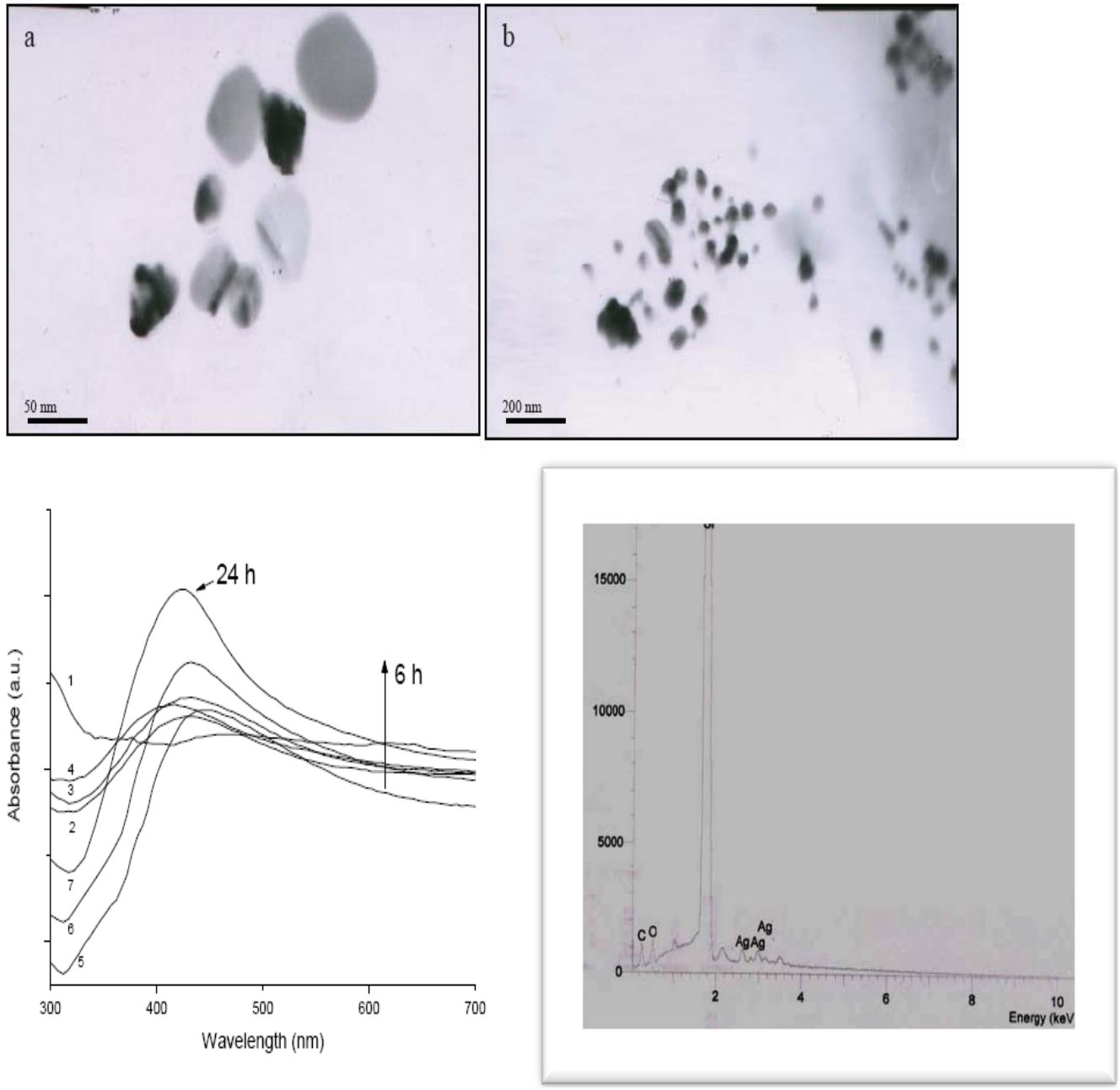

Figure 5. UV-Vis spectra, EDAX and HR-TEM micrograph of synthesized Ag nanoparticles (20-80 Nanometers; spherical and triangle shaped) by *Terminalia* leaf extract.

interesting to note that most of the particles in the TEM pictures are not in physical contact but are separated by a fairly uniform inter-particle distance. From the higher magnification TEM images (Figure 8D) it can be seen that each silver nanoparticle is surrounded by a material with a lower contrast as indicated by an arrow for one of the particles. We believe that this coating material with an average thickness of 5 nm is a bioorganic component of the *T. catappa* extract acting as a stabilizing agent for the nanoparticles. Figure 9 shows TEM images recorded for the Silver Nano Bio Conjugates synthesized by treating $AgNO_3$ solution with *E. officinalis* extract. The silver nanoparticles are observed to range in size from 10 to 30 nm with an average size of ca. 15 nm (Figure 9A).

The morphology of the Ag nanoparticles is predominantly spherical. Few of the particles indicated by the arrows in Figure 9B, appear to have core shell like structure. As stated before, morphology of some of the particles appear to be disc like, while an exact estimate of the thickness of these apparent flat, disc-like particles

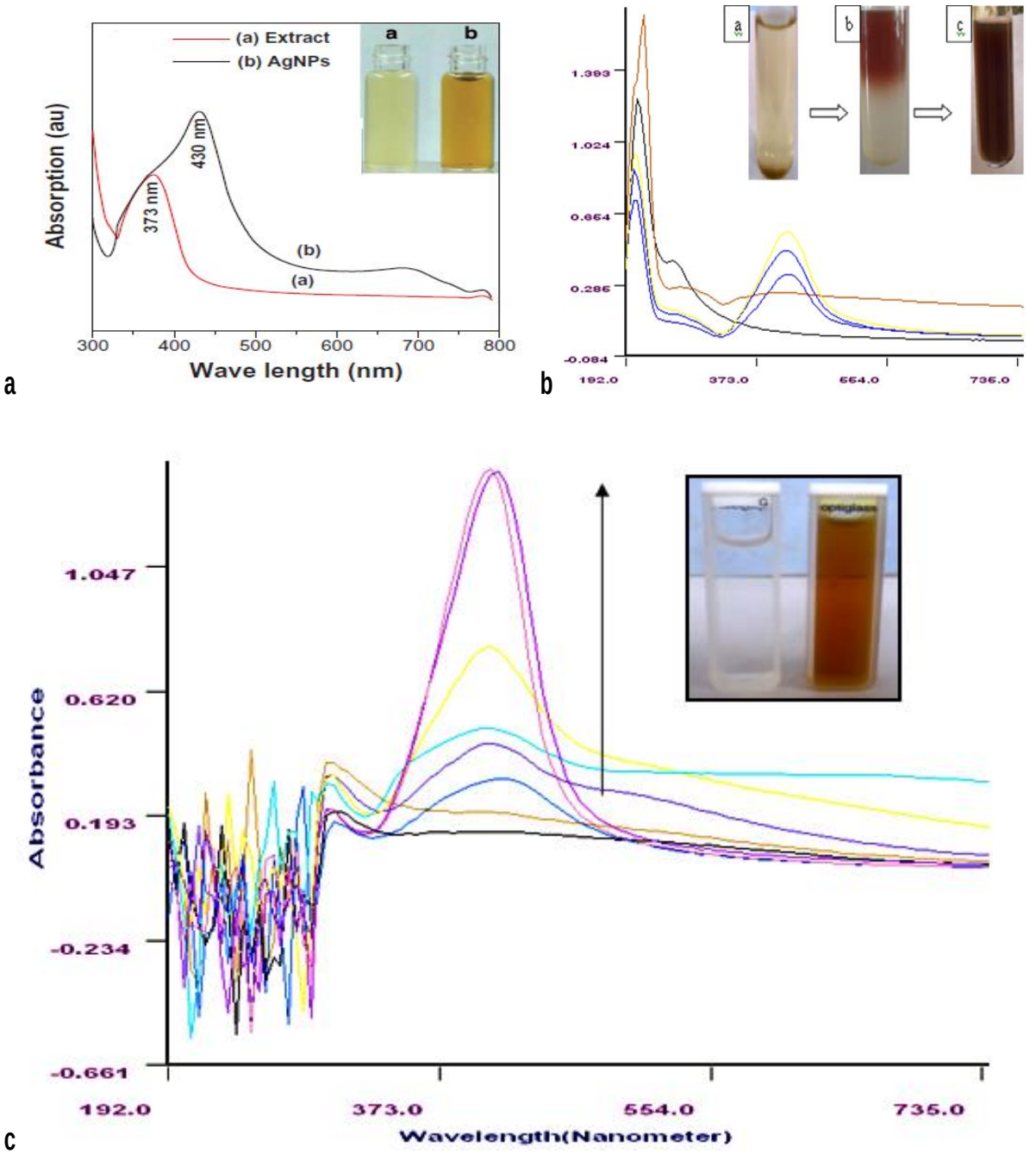

Figure 6. Shows the UV-vis spectra recorded as a function of time of reaction of Ag+ ions with *Emblica officinalis, Eucalyptus hybrida* and *Terminalia catappa* extract. The band corresponding to the surface Plasmon vibrations of Ag nanoparticles is observed at 430 nm. The intensity of the surface plasmon band is seen to saturate after 2 h of reaction. **(a)** UV-vis *spectra of Emblica officinalis* extract, **(b)** UV-vis *spectra of Eucalyptus hybrid* extract, **(c)** UV-vis *spectra of Terminalia catappa* extract.

could not be made; the fact that the thickness of these structures is less than that of the spherical particles is inferred from the increased contrast in places where such nanoparticles overlap. A typical TEM image of silver nano bio conjugates (Figure 10a and b) revealed the presence of maximum number of spherical shapes. The average diameter of 252 particles measured in TEM was 11.10 ± 6.40 nm. A high resolution TEM (HRTEM) image of Silver Nano Bio Conjugates synthesized by eucalyptus (Figure 10c) showed the well resolved interference fringe patterns separated by 0.24 nm which corresponded well to the spacing between (111) plane of fcc silver crystal

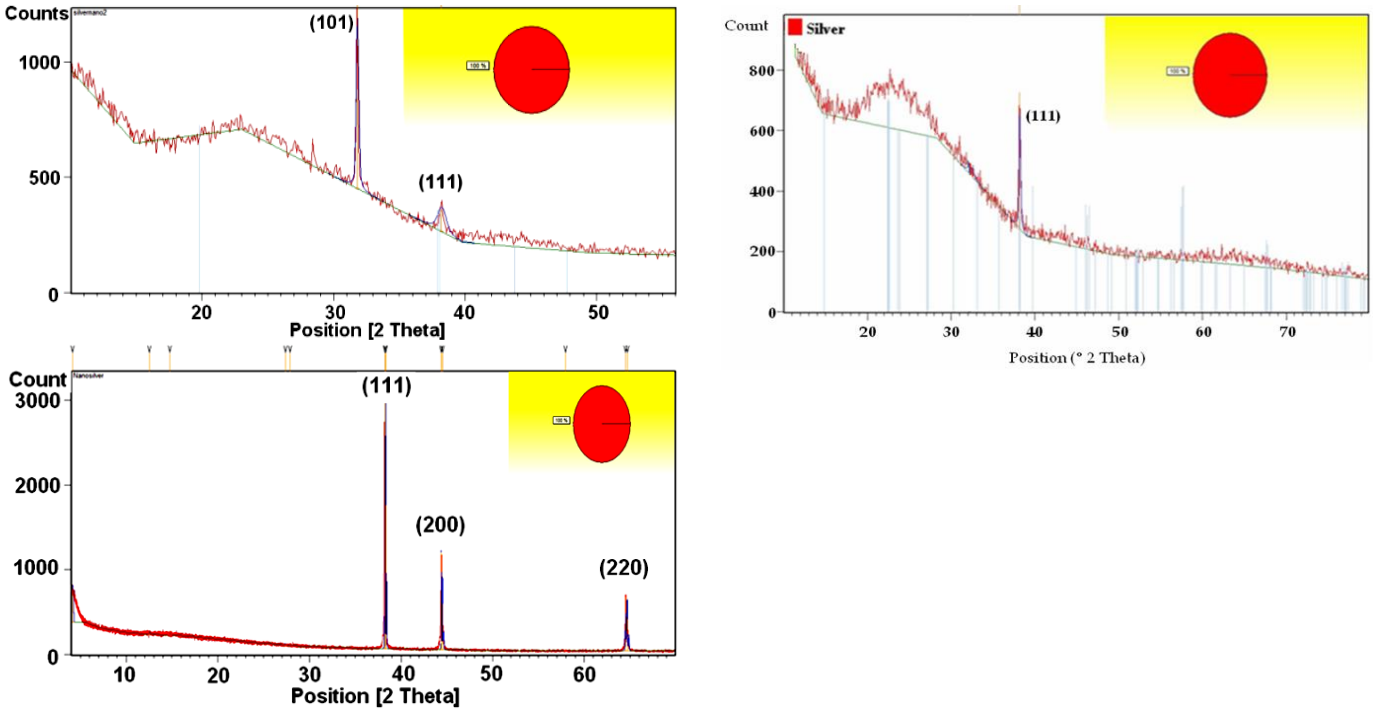

Figure 7. XRD patterns recorded from drop-coated films on glass substrate of silver nanoparticles synthesized by treating *Emblica officinalis, Eucalyptus hybrida* and *Terminalia catappa* leaf extract with $AgNO_3$ aqueous solutions.

Table 1. Lattice spacing values calculated from the 2θ values obtained from the XRD pattern of silver nanoparticles synthesized using *Terminalia catappa* leaf, Eucalyptus hybrid and *Emblica officinalis*.

Pos. [°2Th.]	Lattice Planes (hkl)	Standard Ag (A^o)	*Terminalia catappa* -Ag (A^o)	*Emblica officinalis* Ag (A^o)	*Eucalyptus A*g (A^o)
32	(101)	2.815	-	2.81446	-
38	(111)	2.359	2.35291	2.35567	2.2111
45	(200)	2.044	2.03897	-	-
65	(220)	1.445	1.44446	-	-

(JCPDS. No.01-087-0597). The patterns of SAED (Figure 10d) were indexed according to (111), (200), (220) and (311) reflections of fcc silver crystal on the basis of their d-spacing of 2.47, 2.13, 1.49 and 1.27 A°.

Energy diffraction X- ray (EDX) measurements

The EDX analysis was carried out using JEOL JSM 7600F. Figure 11 shows the energy dispersive analysis by X- rays (EDAX) spectrum of the plain *T. catappa* and *E. officinalis* extract and it is observed that the both extract consists of a number of inorganic ions apart from the presence of carbon and oxygen originating from the bioorganic component of the extract. *T. catappa* leaf extract and *E. officinalis* extract also contains potassium, calcium and magnesium in appreciable amounts. Presence of magnesium possibly indicates that the extract also consists of considerable amount of chlorophyll in it. Figure 12 shows the energy dispersive analysis by X- rays (EDAX) spectrum of the silver nano bioconjugates from *T. catappa* leaf and *E. officinalis* extract confirming the presence of elemental silver signal of silver nanoparticles. The vertical axis displays the number of x-ray counts whilst the horizontal axis displays energy in KeV. Identification lines for the major emission energies for silver (Ag) are displayed and these correspond with peaks in the spectrum, thus giving confidence that silver has been correctly identified.

Fourier transform infrared (FTIR) spectroscopy

Components from *T. catappa* leaf showed that alkaloids,

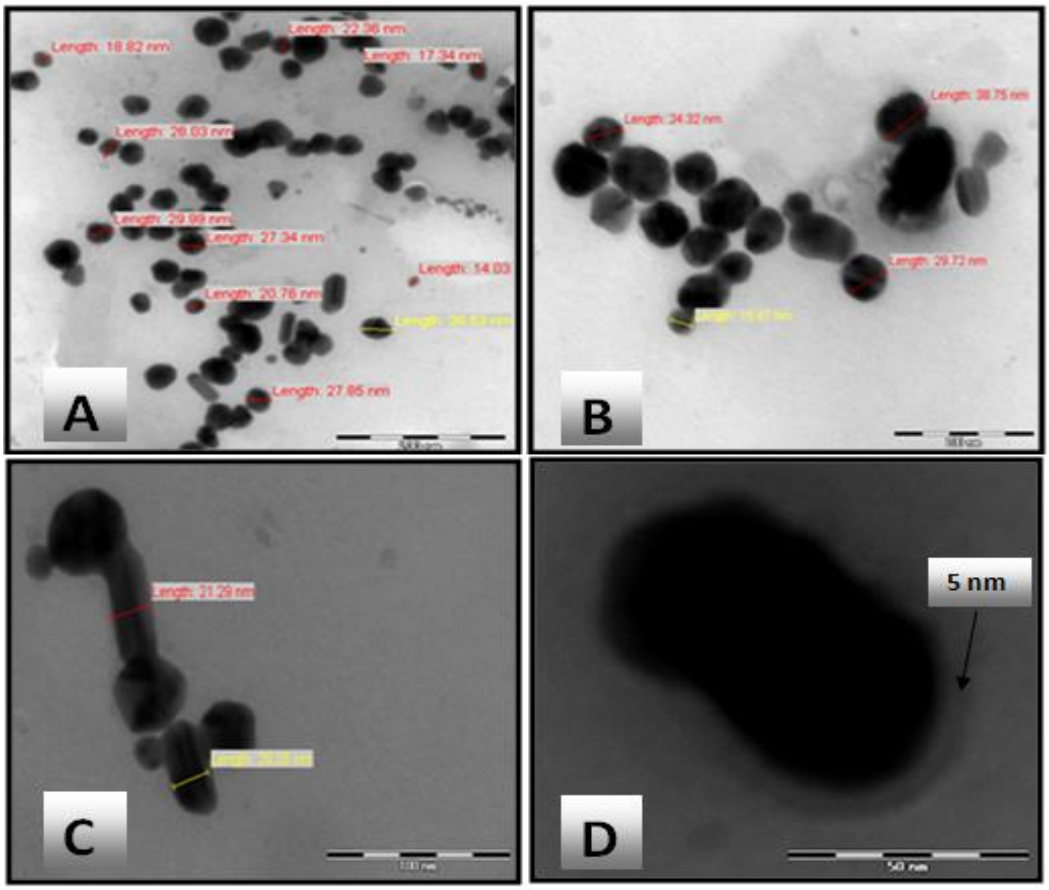

Figure 8. TEM images of silver nano bio conjugates synthesized by *Terminalia catappa* extract.

tannin, flavonoid, and glycosides exist in leaf. FTIR absorption spectra of the dried biomass of *T. catappa* leaf before and after bioreduction, are shown in Figure 13 (i); other information regarding the chemical change of the functional groups were involved in bioreduction. Some absorbance bands centred at 1109, 1244, 1317, 1384, 1446, 1517, 1631 and 1726 cm^{-1} were observed in the region 1000 to 1800 cm^{-1}. Among them, the absorbance bands at 1109, 1631 and 1726 cm^{-1} were associated with the stretch vibration of –C–O, –C=C, RHC=O, respectively. To a large extent, the band at 1109 cm^{-1} might be contributed by the –C–O groups of the polyols such as flavones and polysaccharides in the biomass. It could be figured out by comparison of (a), and (b) that the disappearance of the band at 1109 cm^{-1} after bioreduction shows that the polyols are mainly responsible for the reduction of silver ions. For silver nanoparticles, the absorption at about 1384 cm^{-1} (a) was notably enhanced in that NO^{-3} existed in the residual solution. To a large extent, the bonds or functional groups, such as –C–O–C–, –C–O–, –C=C– and –C=O, derive from the heterocyclic compounds that are water-soluble components in biomass. Therefore, it is thought that the water soluble heterocyclic compounds, for example, alkaloids and flavones, are the capping ligands of the nanoparticles.

FTIR absorption spectra of *E. officinalis* extract before and after reduction of silver are shown in Figure 13 (ii). Extract shows hydroxyl group in alcoholic and phenolic compound which is supported by the presence of a strong peak at approximately 3300 cm^{-1}. This sharp peak representing O–H bond is not seen in *E. officinalis* extract after bioreduction. This indicates that the polyols are mainly responsible for reduction of Ag+ into silver nanoparticles. This may lead to the disappearance of the O–H bond. We could observe free hydroxyl groups in the FTIR of silver nanoparticles at 3600 cm^{-1}. The absorbance bands at 2931, 1625, 1404 and 1143 cm^{-1} are associated with the stretch vibrations of alkyl C–C, conjugated C–C with a benzene ring, bending of C–O–H and C–O stretch in saturated tertiary or secondary highly symmetric alcohol in *E. officinalis* extract, respectively. The presence of peaks at 3749 and 1523 cm^{-1} indicate that the silver nanoparticles may be surrounded by amines, because the peaks indicate $–NH_2$ symmetric stretching and N–O bonds in nitro compounds. The intense broad band at 3384 cm^{-1} is due to the O−H stretching mode and at 2921 cm^{-1} due to the aldehydic

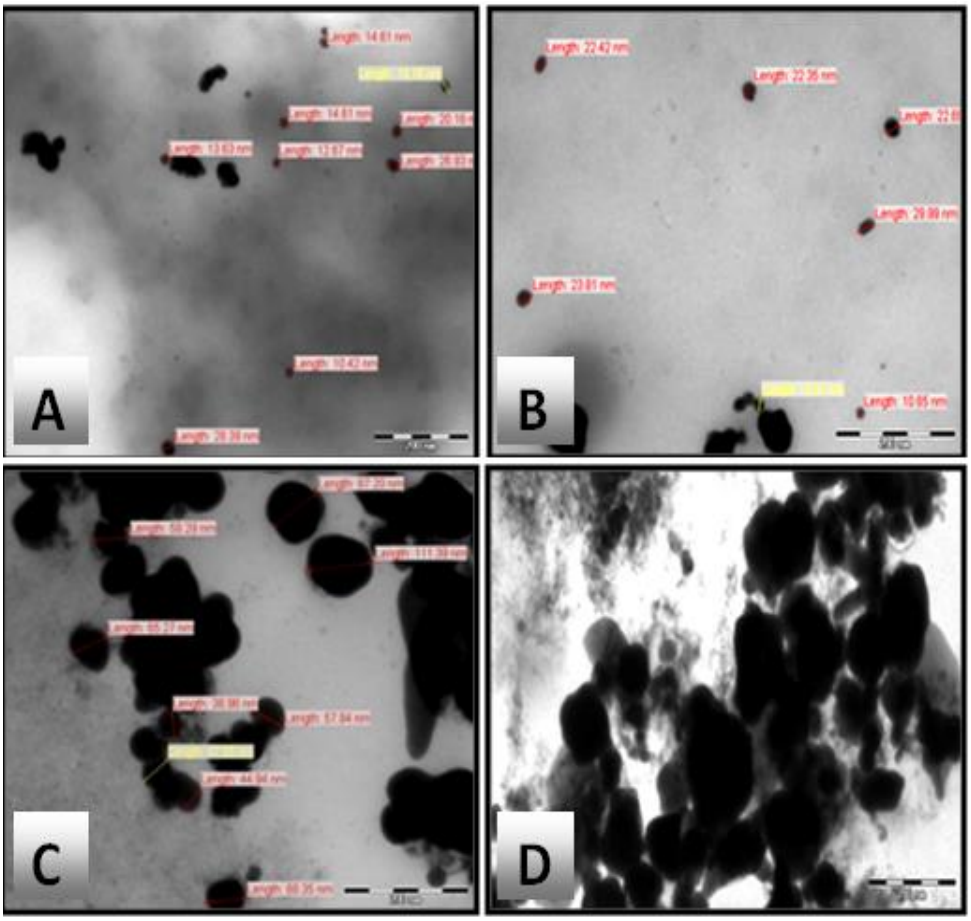

Figure 9. TEM images of Silver Nano Bio Conjugates synthesized by *Emblica officinalis* extract.

C−H stretching mode. The peak at 1078 cm^{-1}, which is absent for the AgNP FTIR spectrums, is the bending vibration of the C−O stretch and could be due to the stabilization of AgNP through this group. The peak of C=C group (at 1406 cm^{-1}) absent for AgNP is possible, due to the reduction of $AgNO_3$ to Ag. It is corresponding to the results of the UV-vis spectroscopy that the extract played a role as the reducing and stabilizing agent in the preparation of AgNP. This indicated the presence of extracts as a capping agent for AgNP, which increases the stability of the nanoparticles synthesized.

In the present scenario, Ag-NPs as antibacterial agents have come up as a promising candidate in the medical field (Duran et al., 2007). The extremely small size of nanoparticles exhibits enhanced or different properties when compared with the bulk material. There are different physical and chemical methods (Chen et al., 2003) for the synthesis of nanoparticles, but there is always need for the development of eco-friendly route for the synthesis process (Ingle et al., 2008). Hence, our current study proves to be an important step in this direction. In the current work of synthesis of Ag- NPs using plant leaf extracts, the colour of the filtrate changed from pale yellow to dark brown after addition of silver nitrate (1 $mmol^{-1}$). Our results show resemblance to that reported by Gade et al. (2008), who reported the formation of brown colour of the cell filtrate of *Aspergillus niger* after treatment with silver nitrate (1 $mmol^{-1}$).

The UV-Vis spectrophotometer analysis showed the absorbance at around 440 nm in the form of sharp peak, which was specific for the synthesis of Ag-NPs; these findings corroborate with the findings of Wang et al. (2007) who reported the same results, in which they observed that when *Capsicum annum* L. extract was challenged with aqueous silver ions, the reaction mixture containing Ag-NPs showed the absorption peak at about 440 nm because of the excitation of longitudinal Plasmon resonance vibration.

In similar study, silver nanoparticles were synthesized using flower broth of *Tagetes erecta* as reductant by a simple and eco-friendly route. The aqueous silver ions when exposed to flower broth were reduced and resulted in green synthesis of silver nanoparticles. The silver nanoparticles were characterized by UV-visible spectroscopy, zeta potential, Fourier transform infra-red spectroscopy (FTIR), X-ray diffraction, transmission

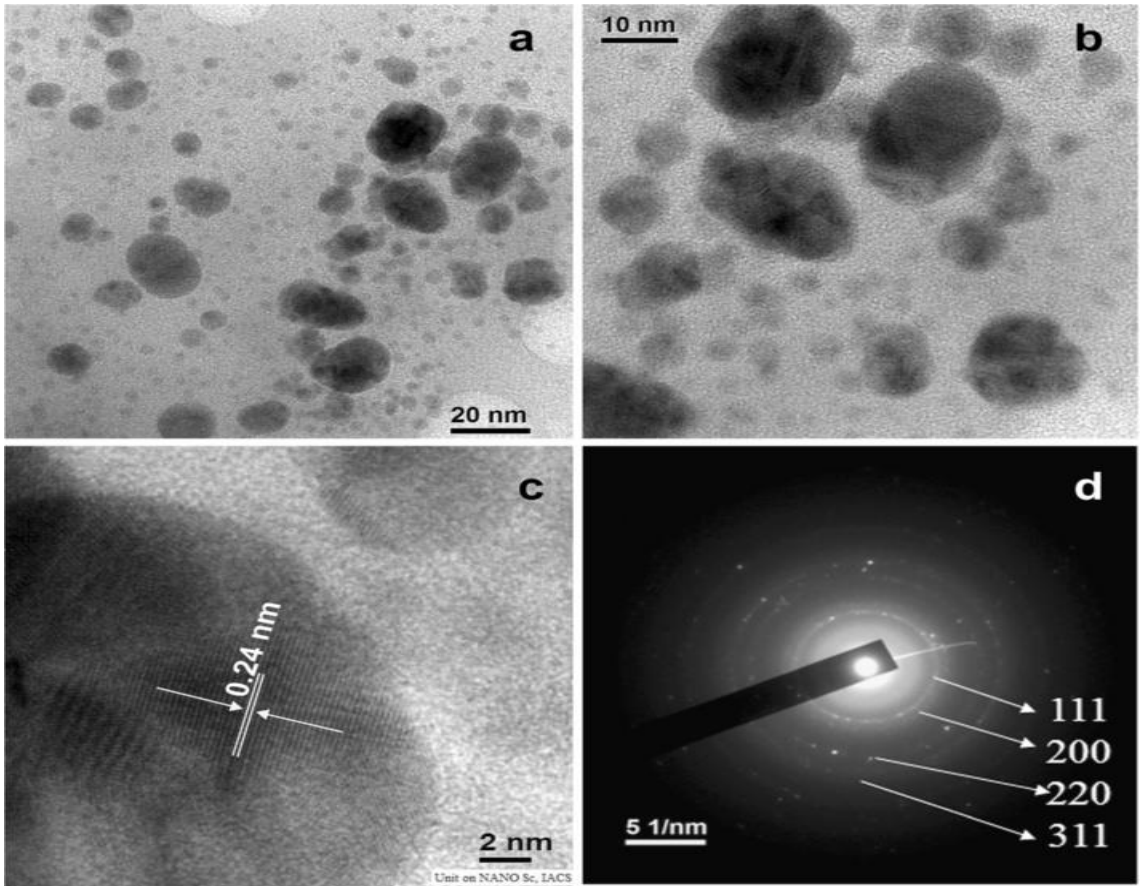

Figure 10. TEM images of silver nano bio conjugates synthesized by *Eucalyptus hybrid* extract.

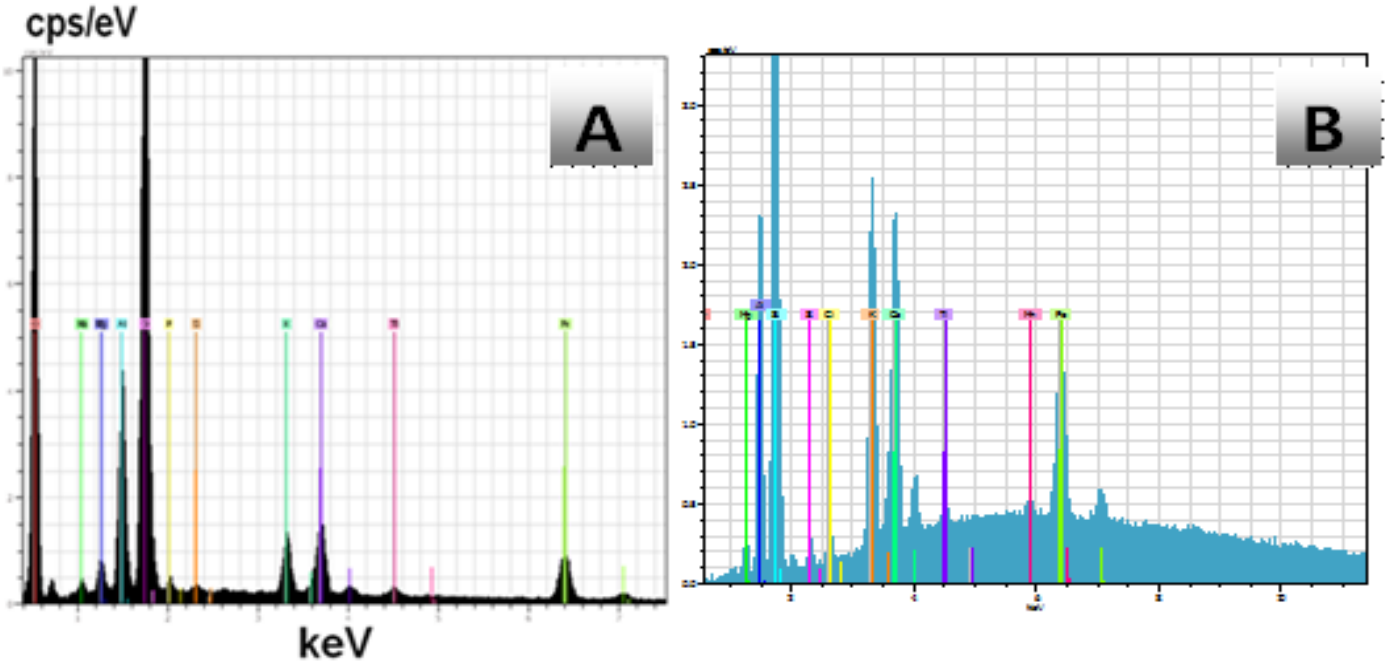

Figure 11. EDX of crude extract of (A) *Terminalia catappa* and (B) *Emblica officinalis* in absence of any external additive.

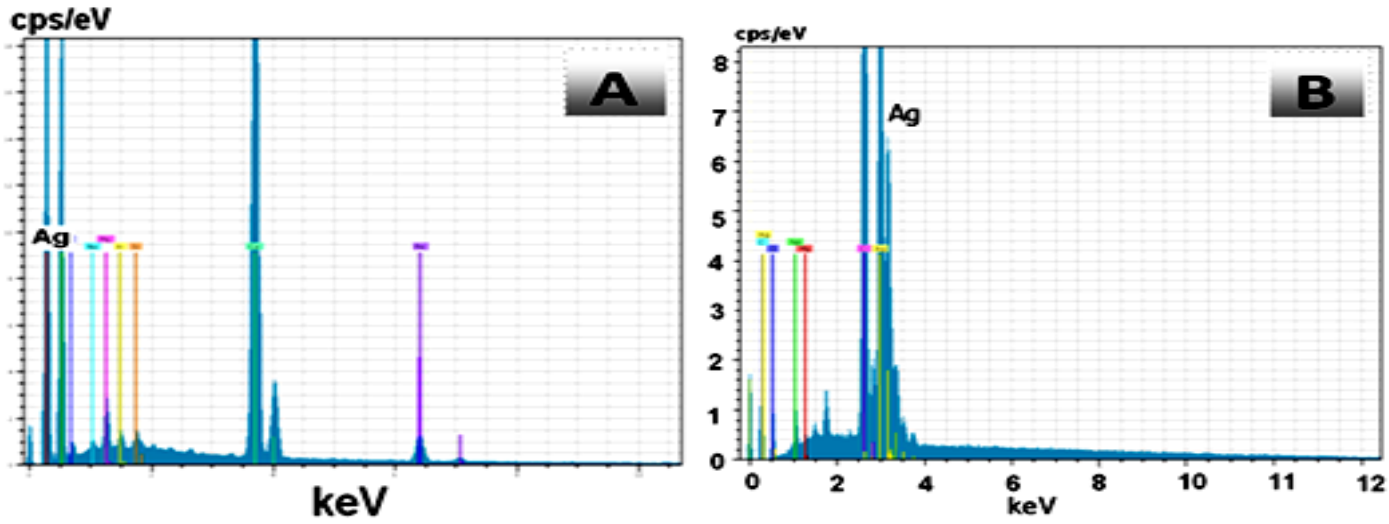

Figure 12. EDX spectrum recorded from a film, after formation of silver nano bioconjugates from (A) *Terminalia catappa* and (B) *Emblica officinalis* extract. Different X-ray emission peaks are labeled.

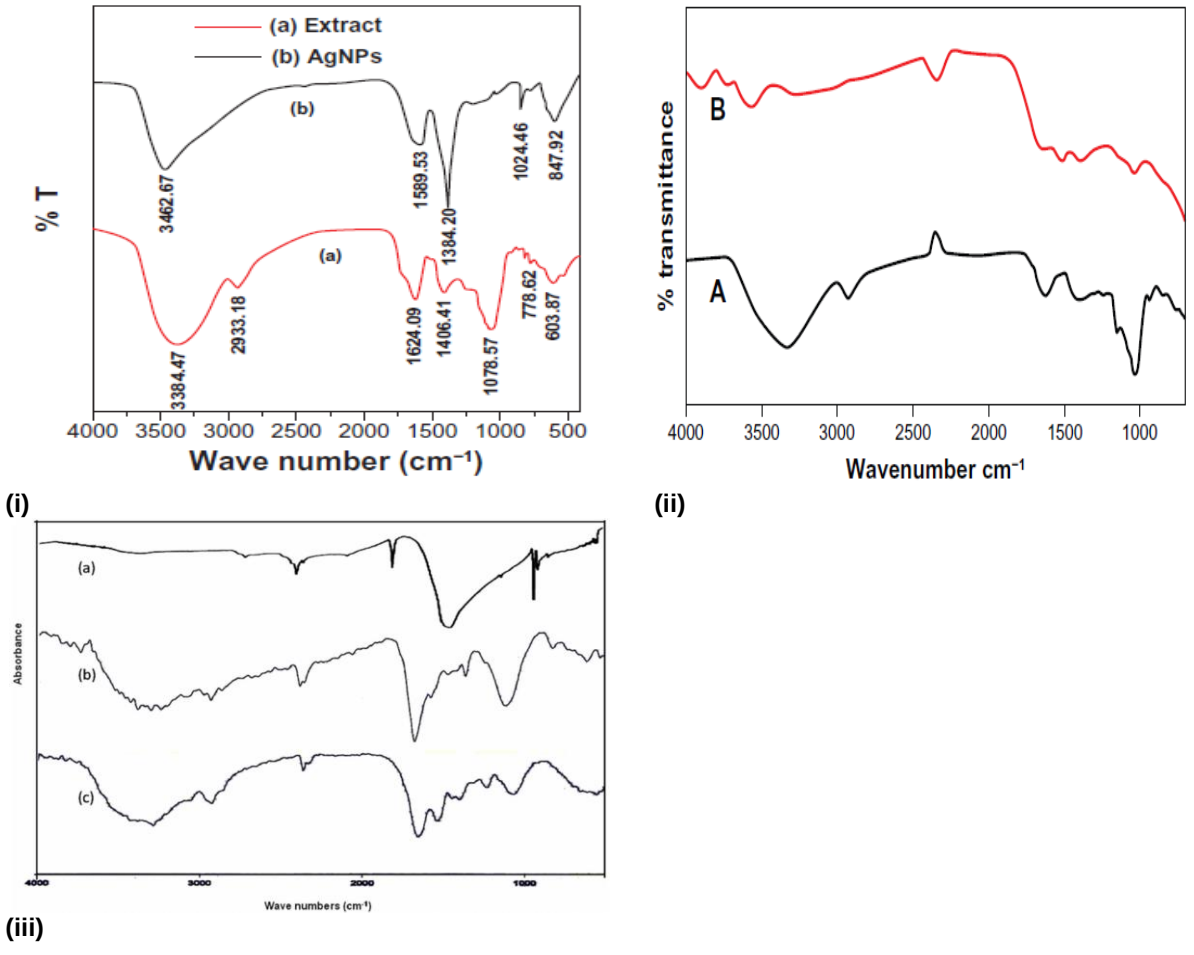

Figure 13. Typical FTIR absorption spectra of the (i) *Terminalia catappa* leaf biomass before bioreduction (a), after bioreduction of silver ions (b). (ii*) Emblica officinalis* biomass before bioreduction (a), after bioreduction of silver ions (b). (iii) Fourier transform infrared absorption spectra of Eucalyptus hybrida extract (A) $AgNO_3$, (b) before bioreduction and (c) after complete bioreduction of Ag+ ions at 50°C.

electron microscopy (TEM) analysis, Energy dispersive X-ray analysis (EDX) and selected area electron diffraction (SAED) pattern. UV–visible spectrum of synthesized silver nanoparticles showed maximum peak at 430 nm. TEM analysis revealed that the particles were spherical, hexagonal and irregular in shape and size ranging from 10 to 90 nm and Energy dispersive X-ray (EDX) spectrum confirmed the presence of silver metal. Synergistic antimicrobial potential of silver nanoparticles was evaluated with various commercial antibiotics against Gram positive (*Staphylococcus aureus* and *Bacillus cereus*), Gram negative (*E. coli* and *Pseudomonas aeruginosa*) bacteria and fungi (*Candida glabrata, Candida albicans, Cryptococcae neoformans).* The antifungal activity of AgNPs with antibiotics was better than antibiotics alone against the tested fungal strains and Gram negative bacteria, thus signification of the present study is in production of biomedical products (Hemali et al., 2014).

AgNPs from *Annona squamosa* leaf extract were spherical in shape with an average size ranging from 20 to 100 nm (Vivek et al., 2012) while Thirunavokkarasu et al. (2013) reported spherical nanoparticles with size ranging from 8 to 90 nm in *Desmodium gangeticum*. The sharp signal peak of silver strongly indicated the reduction of silver ion by *T. erecta* into elemental silver. Metallic silver nanoparticles generally show typical optical absorption peak approximately at 2.6 keV due to surface plasmon resonance. There were spectral signals for C and Cu because of the TEM grid used. From EDX spectrum, it was clear that *T. erecta* had percent yield of 71.31% of AgNPs and synthesized nanoparticles were composed of high purity AgNPs. TEM images showed that the surfaces of the AgNPs were surrounded by a black thin layer of some material which might be due to the capping organic constituents of flower broth as also reported by Rafiuddin (2013).

Thakur et al. (2013) and Niraimathi et al. (2013) also reported antibacterial activity of AgNPs. The AgNPs plus antibiotics could successfully inhibit the fungal strains under investigation while acetone extract plus antibiotics could not. Antifungal activity of AgNPs with commercial antibiotics is also reported by Kim et al. (2009) and Gajbhiye et al. (2009). However, they have reported against only fungi and only with two antibiotics, that is, fluconazole and amphotericin B, respectively. The mechanism of inhibitory effects of silver ions on microorganisms is somewhat known. Some studies have reported that positive charge on the silver ion is significant for its antimicrobial activity through the electrostatic attraction between negative charge on cell membrane of microorganism and positive charged nanoparticles (Hamouda and Baker, 2000; Dibrov et al., 2002; Chanda, 2014).

In the FTIR analysis, the amide linkages between amino acid residues in proteins give rise to the well-known signatures in the infrared region of the electro-magnetic spectrum. Representative spectra of obtained nanoparticles manifest absorption peaks in the region 1000 to 2000 cm^{-1}. Among them, the absorption peak at around 1025 cm^{-1} can be assigned as absorption peaks of –C–O–C– or –C–O– (Huang et al., 2007). The peak at 1630 cm^{-1} is associated with stretch vibration of –C=C– (Huang et al., 2007) and is assigned to the amide I bonds of proteins (Sastry et al., 2003) in the present FTIR spectrum. The SEM micrograph study showed the presence of spherical nanoparticles in the range of 60 to 80 nm, and aggregates of silver nanoparticles were also observed in the micrograph; these findings corroborate the observations of Sadowski et al. (2008) that the nanoparticles get partially aggregated because of the drying process. However, future studies on antibacterial activity of the influence of these nanoparticles on other Gram-positive and Gram negative bacteria are necessary in order to evaluate it as a better bactericidal material.

Conclusion

In the present study, plant extracts were studied for the synthesis of Ag-NPs. We have reported a simple biological process for synthesizing Ag-NPs. The FTIR analysis confirms capping over Ag-NPs. These capped Ag-NPs will help to enhance the stability of Ag-NPs in a colloidal solution by preventing aggregation of particles. Because they are capped by biomolecules and they may serve as a better candidate for the drug delivery systems. However, synthesis of nanoparticles using plant extracts can potentially eliminate the problem of chemical agents, which may have adverse effects in its application, thus making nanoparticles more biocompatible.

Conflict of interests

The authors did not declare any conflict of interest.

Abbreviations: XRD, X-Ray diffraction; **Ag-NPs,** silver nanoparticles; NT, nanotechnology; **TEM,** transmission electron microscopy; **EDX,** energy diffraction X- ray; **FFT,** fast Fourier transform; **FTIR,** Fourier transform infrared spectroscopy; **SAED,** selected area electron diffraction.

REFERENCES

Catauro M, Raucci MG, De Gaetano FD, Marotta A (2004). Antibacterial and bioactive silver-containing Na2O CaO 2SiO2 glass prepared by sol-gel method. J. Mater. Sci. Mater. Med. 15(7):831-837.

Chanda S (2014). Silver nanoparticles (medicinal plants mediated): a new generation of antimicrobials to combat microbial pathogens – a review. In: Mendez-Vilas, A. (Ed.), Microbial Pathogens and Strategies for Combating Them: Science Technology and Education. FORMATEX Research Center, Badajoz, Spain. pp. 1314-1323.

Chen JC, Lin ZH, Ma XX (2003). Evidence of the production of silver nanoparticles via pretreatment of *Phoma* sp. 3Æ2883 with silver nitrate.

Lett . Appl. Microbiol. 37:105-108.
Crabtree JH, Burchette RJ, Siddiqi RA, Huen IT, Handott LL, Fishman A (2003). The efficacy of silver-ion implanted catheters in reducing peritoneal dialysis-related infections. Perit. Dial. Int. 23(4):368-374.
Dibrov P, Dzioba J, Gosink KK, Hase CC (2002). Chemiosmotic mechanism of antimicrobial activity of Ag (+) in *Vibrio cholera*. Antimicrob. Agents Chemother. 46: 2668-2670.
Duran N, Alves OL, De Souza GIH, Esposito E, Marcato PD (2007). Antibacterial effect of silver nanoparticles by fungal process on textile fabrics and their effluent treatment. J. Biomed. Nanotechnol. 3:203-208.
Gade AK, Bonde PP, Ingle AP, Marcato PD, Duran N, Rai MK (2008). Exploitation of *Aspergillus niger* for fabrication of silver nanoparticles. J. Biobased Mater. Bioenergy 2:243-247.
Gajbhiye M, Kesharwani J, Ingle A, Gade A, Rai M(2009). Fungus-mediated synthesis of silver nanoparticles and their activity against pathogenic fungi in combination with fluconazole. Nanomed. NBM 5:382-386.
Gonzalez AL, Noguezm C (2007). Influence of Morphology on the Optical Properties of Metal Nanoparticles. J. Comput. Theor. Nano-sci. 4 (2): 231-238.
Gross M, Winnacker MA, Wellmann PJ (2007). Electrical, Optical and Morphological Properties of Nanoparticle Indium-Tin-Oxide Layers. Thin Solid Films 515 (24): 8567-8572.
Hamouda T, Baker JR (2000). Antimicrobial mechanism of action of surfactant lipid preparations in enteric Gram-negative bacilli. J. Appl. Microbiol. 89:397-403.
Hemali P, Pooja M, Sumitra C (2014). Green synthesis of silver nanoparticles from marigold flower and its synergistic antimicrobial potential. Arabian J. Chem. (In Press).
Huang J, Chen C, He N, Hong J, Lu Y, Qingbiao L, Shao W, Sun D et al. (2007). Biosynthesis of silver and gold nanoparticles by novel sundried Cinnamomum camphora leaf. Nanotechnology 18:105-106.
Ingle A, Gade A, Pierrat S, Sonnichsen C, Rai M (2008). Mycosynthesis of silver nanoparticles using the fungus *Fusarium acuminatum* and its activity against some human pathogenic bacteria. Curr. Nanosci. 4:141–144.
Jones SA, Bowler PG, Walker M, Parsons D (2004). Controlling wound bioburden with a novel silver-containing Hydrofiber dressing. Wound Repair Regen. 12 (3):288-294.
Kim JY, Kim M, Kim HM, Joo J, Choi JH (2003). Electrical and Optical Studies of Organic Light Emitting Devices Using SWCNTs-Polymer Nanocomposites. Opt. Mater. 21 (1-3):147-151.
Kim KJ, Sung WS, Suh BK, Moon SK, Choi JS, Kim JG, Lee DG (2009). Antifungal activity and mode of action of silver nano-particles on Candida albicans. Biometals 9(22):235-242.
Mihail CR (2003). Nanotechnology: convergence with modern biology and medicine. Curr. Opin. Biotechnol. 14:337-346.
Niraimathi KL, Sudha V, Lavanya R, Brindha P (2013). Biosynthesis of silver nanoparticles using Alternanthera sessilis (Linn.) extract and their antimicrobial, antioxidant activities. Colloids Surf. B Biointerfaces 102:288-291.
Parak WJ, Gerion D, Pellegrino T, Zanchet D, Micheel C, Williams SC, Boudreau R, Le Gros MA, Larabell CA, Alivisatos AP (2003). Biological Applications of Colloidal Nanocrystals. Nanotechnology 14(7):15-27.
Rafiuddin ZZ (2013). Bio-conjugated silver nanoparticles from Ocimum sanctum and role of cetyltrimethyl ammonium bromide. Colloids Surf. B Biointerfaces 108:90-94.
Sadowski Z, Maliszewska IH, Grochowalska B, Polowczyk I, Kozlecki T (2008). Synthesis of silver nanoparticles using microorganisms. Mater. Sci. Pol. 26:419-425.
Sastry M, Ahmad A, Khan MI, Kumar R (2003). Biosynthesis of metal nanoparticles using fungi and actinomycetes. Curr. Sci. 85: 162–170.
Schultz DA (2003). Plasmon Resonant Particles for Biological Detection. Curr. Opin. Biotechnol. 14(1):13-22.
Silver S, Phung LT (1996). Bacterial heavy metal resistance: new surprises. Annu. Rev. Microbiol. 50:753- 89.
Smith AM, Duan H, Rhyner MN, Ruan G, Nie S (2006). A Systematic Examination of Surface Coatings on the Optical and Chemical Properties of Semiconductor Quantum Dots. Phys. Chem. Chem. Phys. 8(33):3895-3903.
Stevanovic MM, Skapin SD, Bracko I, Milenkovic M, Petkovic J, Filipic M (2012). Poly (lactide-co-glycolide)/silver nanoparticles: synthesis, characterization, antimicrobial activity, cytotoxicity assessment and ROS-inducing potential. Polymer 53:2818-2828.
Thakur M, Pandey S, Mewada A, Shah R, Oza G, Sharon M (2013). Understanding the stability of silver nanoparticles biofabricated using Acacia arabica (Babool gum) and its hostile effect on microorganisms. Spectrochim. Acta Part A Mol. Biomol. Spectrosc. 109: 344–347.
Thirunavokkarasu M, Balaji U, Behera S, Panda PK, Mishra BK (2013). Biosynthesis of silver nanoparticles from extract of Desmodium gangeticum (L.) DC. and its biomedical potential. Spectrochim. Acta Part A Mol. Biomol. Spectrosc. 116:424-427.
Vivek R, Thangam R, Muthuchelian K, Gunasekaran P, Kaveri K, Kannan S (2012). Green biosynthesis of silver nanoparticles from Annona squamosa leaf extract and its in vitro cytotoxic effect on MCF-7 cells. Process Biochem. 47:2405-2410.
Wang HY, Li YF, Hua CZ (2007). Detection of ferulic acid based on the plasmon resonance light scattering of silver nanoparticles. Special Issue on China Japan-Korea Environmental Analysis, Talanta 72(5):1698-1703.
Wei GH, Zhou Z, Liu Z. (2005). A Simple Method for the Preparation of Ultrahigh Sensitivity Surface Enhanced Raman Scattering (SERS) Active Substrate. Appl. Surf. Sci. 240(1-4): 260-267.
Yamanaka M, Hara K, Kudo J (2005). Bactericidal actions of a silver ion solution on Escherichia coli, studied by energy-filtering transmission electron microscopy and proteomic analysis. Appl. Environ. Microbiol. 71:7589-7593.
Zhao G, Stevens Jr SE (1998). Multiple parameters for the comprehensive evaluation of the susceptibility of *Escherichia coli* to the silver ion. Biometals 11:27-32.